Catalysis Today 440 (2024) 114849

Contents lists available at ScienceDirect

Catalysis Today

journal homepage: www.elsevier.com/locate/cattod

Biogas upgrading through CO_2 methanation in a polytropic - distributed feed fixed bed reactor

P. Durán [a], P. Aragüés-Aldea [a], R. González-Pizarro [a], V.D. Mercader [a], F. Cazaña [b], E. Francés [a], J. A. Peña [a], J. Herguido [a,*]

[a] Catalysis and Reactor Engineering Group (CREG) - Aragon Institute of Engineering Research (I3A), Universidad Zaragoza, c/ Mariano Esquillor s/n, Zaragoza 50018, Spain

[b] Laboratorio de Microscopías Avanzadas (LMA), Universidad Zaragoza, c/ Mariano Esquillor s/n, Zaragoza 50018, Spain

ARTICLE INFO

Keywords:
CO_2 methanation
Biogas upgrading
Distributed feeding
Ni-Mn catalyst
Power to gas
Improved selectivity

ABSTRACT

Methanation of the CO_2 contained in a biogas stream has been experimentally analyzed in a fixed bed reactor with a Ni-Mn catalyst, evaluating the effect of feeding reactants distributed throughout the bed. The performance of different feeding configurations (conventional cofeeding and others implying a lateral distribution of one of the reactive streams) has been analyzed for different nominal temperatures *T* (250–400 ºC) and weight-related space velocities *WHSV* (47.71–6.63 $g_{CO2}\ g_{cat}^{-1}\ h^{-1}$), always keeping a H_2: CO_2 ratio of 4:1, and a CH_4:CO_2 ratio of 7:3. For identical *WHSV,* the lateral biogas distribution (*Poly-Biogas* feeding configuration) always showed the best results in terms of activity (higher conversion at the same temperature) and selectivity (lower selectivity to CO in iso-conversion). These better results agree with what was observed in a previous work in methanation of CO_2 (i.e., without methane in the feed). In that work, CO_2 was distributed along the catalytic bed by several lateral feeds (*Poly-CO_2*). When *T* was kept constant and *WHSV* was varied, the reactor fed with distributed biogas (*Poly-Biogas*), again confirmed its higher efficiency and better selectivity for biogas upgrading (i.e., higher CH_4 content). Furthermore, by adopting a *Poly-Biogas* (or *poly-CO_2*) feeding configuration, a more homogeneous temperature profile was achieved along the bed avoiding the severity of hot spots appearance. In contrast, the lateral distribution of hydrogen (*Poly-H_2*) always led to similar or worse results than those for the conventional co-feeding configuration.

1. Introduction

The Power-to-Gas (PtG) strategy could play an essential role in the upcoming energy scenario. Hydrogen obtained from surplus renewable electricity, via water electrolysis, would be the energy vector in the PtG process. It can be transformed into methane (i.e., *Synthetic Natural Gas* -SNG-) by subsequent methanation of the carbon dioxide coming from capture and storage of exhaust gases from industrial processes, as well as renewable sources such as a biogas. In this last case, the conversion of CO_2 present in previously sweetened biogas into added CH_4 using renewable-based hydrogen represents an upgrading step prior to its injection into the natural gas grid or its use as fuel. This biogas methanation could serve as a component integrated into the transition from traditional linear energy systems to circular economy ones (e.g., within a wastewater treatment plant), offering more resilient paths [1].

In the last decade, a large number of researchers have revisited PtG technology and a remarkable increase in ongoing projects have started dealing with it [2], being practically all of them based on catalytic fixed bed reactors. However, the high exothermicity of CO_2 methanation (*Sabatier* reaction -r.1-), requires ensuring good temperature control in the bed to prevent hot spots conducting to catalysts sintering and thermodynamic limitations. That is why several novel reactor concepts (e.g., three-phase methanation and micro reactors) are currently under development [3].

$$CO_2 + 4H_2 \rightleftharpoons CH_4 + 2H_2O \quad \Delta H_r^0 = -165.1\left[kJ{\cdot}mol^{-1}\right] \qquad (r.1)$$

The development of active, selective, and stable catalytic materials for this process, has gained momentum in recent years. Special emphasis has been placed on aspects such as the choice of the active metal (alone or combined with others), the contribution of supports (including active supports), the effect of promoters, the influence of preparation methods

* Corresponding author.
E-mail address: jhergui@unizar.es (J. Herguido).

https://doi.org/10.1016/j.cattod.2024.114849
Received 22 January 2024; Received in revised form 22 April 2024; Accepted 27 May 2024
Available online 28 May 2024

and the regulation of catalyst structure to name a few [4].

Certainly, those variables related to the characteristics of the catalyst widely influence the selectivity towards CO in the CO_2 methanation process. Thus, for example, the particle size of an active Ni catalyst can be decisive. In this sense, working with Ni/CeO_2 nanorods, it has been established [5] that medium-sized (10–25 nm) Ni nanoparticles are of optimal size, while smaller promote the selectivity toward CO, and larger ones greatly reduce the available active sites in the surface. For this same reason, the change in the catalyst preparation method can also have a high effect on the CO selectivity. Thus, *Tsiotsias et al.* [6] obtained significantly different selectivities with Ni catalysts supported on sol-gel derived Pr_2O_3-CeO_2, depending on the preparation method used. Working at constant conditions ($WHSV = 25\times10^3$ $cm^3{\cdot}g_{cat}^{-1}{\cdot}h^{-1}$, H_2:CO_2 molar ratio 4:1, atmospheric pressure, and 400 ºC), they reached different CO_2 conversions (roughly 67 %, 71 %, and 73%) depending on the method of preparation of the catalyst support: typical *Pechini* method (Ni/PC), citrate sol-gel method (Ni/CSG) or a modified *Pechini* method (Ni/MPC), respectively. And furthermore, their respective selectivities to CO were also quite different: 4.2 %, 2.3 %, and 1.3 %, respectively.

Naturally, the catalyst composition has also an important effect on the CO selectivity in the CO_2 methanation process. For example, a recent work by *Boukha et al.* [7] analyzes the behavior of nickel-supported hydroxyapatite (Ni/HAP) samples to which have been added different percentages of Ca (up to 4 % by weight). A large effect was observed on activity, but also on CO selectivity. Thus, working at 250 ºC the CO_2 conversion varied from 1 % to 5 % with a notable variation in CO selectivity, from 18 % to 49 %. Even for the optimal formulation [Ni/Ca (2 wt %)/HAP sample] which was found to be stable for a TOS of 90 h maintaining a CO_2 conversion of 72 % (at 350 ºC, $WHSV = 30\times10^3$ $cm^3{\cdot}g_{cat}^{-1}{\cdot}h^{-1}$, and H_2:CO_2 ratio 4:1), a relatively high stable selectivity to carbon monoxide $S_{CO} = 6$ % was found.

Many studies on CO_2 methanation have recently shown how, even if highly active and selective catalysts are used, high selectivities towards CO can be produced when working under specific reaction conditions. In this sense, for example, using a high-performance Ru/Al_2O_3 catalyst and varying its pellet diameter, a progressive worsening of the performances was noticed by *Larghi et al.* [8]. In fact, when working with pellets larger than 800 μm in diameter, a decrease in CO_2 conversion and an increase in CO selectivity was clearly observed, achieving CO selectivities around 70 % for CO_2 conversions in the range of 20 %. Likewise, on the results obtained with this Ru-based catalyst by reducing the contact time, the selectivity to CO pointed at 100 % in the entire temperature range (190 ºC to 350 ºC) working at atmospheric pressure and with a H_2:CO_2 ratio 4:1 [9]. They also observed the same trends on Ni-based catalysts, confirming CO as a key intermediate in the methanation process.

Considering the examples mentioned in the previous paragraphs, it is confirmed that all these factors are of great influence on the selectivity to CO, but the layout of the reactor (gas contact mode, feed configuration, temperature management, etc…) must also be considered. That is why in a previous work [10], a different alternative to the conventional fixed bed reactors was proposed to be tested: the concept of the polytropic-feed reactor (i.e., a fixed bed reactor with several side gas inlets). This configuration had already been used in our research group several decades ago to the lean distribution of oxygen in methane oxidative coupling reaction [11]. Apart from the thermal benefit derived of the controlled rate of reaction due to the lean amount of reactants, the proposed type of reactor was intended to provide an improvement in selectivity to methane. Considering *Sabatier* reaction as a series-parallel combination of two hydrogenation steps (reverse *Water Gas Shift* -r.2-, and reverse *Methane Steam Reforming* -r.3-), there is a successive attack of a compound (CO_2) by a reactive material (H_2). Therefore, the contact type should greatly influence the distribution of products. Certainly, it was found that side distribution of CO_2 leaded to an improvement of performance in terms of both, conversion enhancement at all temperatures and a notable lowering in selectivity to CO [10]. Furthermore, more homogeneous temperature profiles were observed along the bed for the CO_2 distributed feeding configuration.

$$CO_2 + H_2 \rightleftharpoons CO + H_2O \quad \Delta H_r^0 = +41.2\left[kJ{\cdot}mol^{-1}\right] \tag{r.2}$$

$$CO + 3H_2 \rightleftharpoons CH_4 + H_2O \quad \Delta H_r^0 = -206.3\left[kJ{\cdot}mol^{-1}\right] \tag{r.3}$$

In addition to the aforementioned reactions (r.1, r.2, and r.3), the simultaneous appearance of others raises an additional problem of coke formation in the process. Thus, the exothermic reactions of CO disproportionation (reverse *Boudouard* reaction) and CO hydrogenation, as well as the endothermic reactions of methane decomposition and CO_2 hydrogenation generate carbonaceous residue as a product. In biogas upgrading processes like in others as methane steam reforming or dry reforming, carbon deposition plays an important role at working temperatures. This is important to determine quantity, structure and morphology of the carbonaceous materials deposited on the catalysts exposed to reaction [12,13]. However, when biogas upgrading is carried out through CO_2 methanation, coke production is only favored at high temperature, low pressure and a high CH_4/CO_2 ratio. For example, a thermodynamic analysis of the CO_2 methanation reaction with in situ water removal for biogas upgrading [14] reports that coke formation can be avoided if biogas upgrading via the *Sabatier* reaction is carried out at temperatures lower than 300 °C or pressures higher than 10 atm.

The purpose of this work is to extend the study to the methanation of a CH_4+CO_2 gas stream simulating a sweetened biogas and to compare it with the former results obtained using a stream of CO_2 free of methane. Thus, the influence of side distributed feeding of CH_4+CO_2 or H_2 has been experimentally tested with the aim of maximizing selectivities towards CH_4 (i.e., minimize selectivities to CO), as well as trying to avoid thermal gradients generated by the high exothermicity of the methanation process. A conceptual sketch of this proposal is shown in Graphical Abstract.

Therefore, the novelty of the study lies in the improvement of biogas upgrading through the implementation of a distributed feed of the treated stream. The aim is to achieve a significant reduction in selectivity towards unwanted byproducts of CO_2 methanation (CO and carbonaceous deposits) while maintaining process stability (isothermal behavior of the bed and catalyst stability).

2. Experimental

2.1. Catalyst

A Ni-MnO_x catalyst was chosen for this study based on its high selectivities to CO at a given CO_2 conversion, as deduced from works in which Ni-based catalysts were used supported on biomorphic carbon derived from lignocellulosic biomass residues [15,16]. Reason for that election was the ability of such catalyst for producing the unwanted product (CO) with high selectivity, and consequently increasing the accuracy in its experimental determination. Concretely, a 5 %^{wt} Ni over manganese (III) oxide catalyst was prepared by co-precipitation of both Ni and Mn nitrates using urea, according to a method adapted from *Wei et al.* (2019) [17]. The preparation method detailed elsewhere [10], ended up with a calcination step at 600 ºC for 3 hours, and crushing and sieving the solid to a 100–160 μm particle diameter interval. The catalyst samples were characterized by XRD, BET, XRF, and SEM techniques.

2.2. Reaction setup

Table 1 shows the main operating conditions of the methanation trials, which were performed in this study in a laboratory scale. The experiments were carried out in a fixed bed vertical reactor made of quartz (1.3 cm i.d.) with different side feeding points every 3 cm in height along the 12 cm high bed and an upper main feed [Fig. 1.A]. Different thermocouples were located at these points (heights from the support plate $h_i = 1$, 3, 6, 9, and 12 cm). The temperature profiles (T_1 -

Table 1
Operating conditions.

	standard value	interval
Catalyst load, $W_{cat,0}$ (g)	0.25	0.125 – 0.5
Inert solid load, $W_{inert,0}$ (g)	10.25	10.375 – 10.0
H_2:CO_2 molar ratio	4:1	–
CH_4:CO_2 molar ratio*	7:3	–
Temperature set-point (ºC)	400	400 – 250**
Reagents partial pressure (bar)	0.9	–
WHSV ($g_{CO2}{\cdot}g_{cat}^{-1}{\cdot}h^{-1}$)	13.25	47.71 – 6.63
Total gas flow, q_0 (STP mL/min)	250	62.5 – 450
Particle diameter (μm)	100–160	–

* when feeding biogas
** (-25 °C) intervals (7 temperatures)

T_{12}) were registered over time, using T_6 as the one controlling (PID) an electrical oven housing the reactor. The 5 %^{wt} Ni-MnO_x catalyst was diluted in inert Al_2O_3 (*SASOL Puralox SCCa-150/200*) resulting in 10.5 g total weight of solids in the bed. Prior to methanation, an activation stage was carried out with a H_2 stream (45 ^{v}% Ar, and 5 ^{v}% N_2 as internal standard) at 500 ºC for 2 hours. A total gas flowrate $q_0 = 250$ STP mL·min^{-1}, as standard value, was fed in most experiments, with a composition of 90 ^{v}% of reactive gases, 5 ^{v}% Ar as inert, and 5 ^{v}% N_2 as internal standard. Kinetic control regime was established from previous methanation experiments with dp = 100–160 μm catalyst particle size and q_0 =250 STP mL·min^{-1} feed flow rates. Reactive gases always kept a molar ratio H_2:CO_2 = 4:1, and CH_4:CO_2 = 7:3. Exhaust gases were analyzed by gas micro-chromatography (*Agilent 490 Micro GC*). More details about the experimental procedure can be found elsewhere [10].

Fig. 1B-D show the different feeding configurations adopted in this experimental work. In the conventional configuration (Fig. 1.B) both reactants H_2 and biogas were cofed from the top of the bed. In the configurations with distributed feeding, labelled as 'polytropic' (*Poly-*), a single reactant stream was introduced through the upper front or main entrance (h_{12}) of the reactor, while the second one was distributed homogeneously (i.e., equal flowrates) through the main entrance and side inlets (h_{12}, h_9, h_6, and h_3). Thus, specifically *Poly-H_2* (Fig. 1.C), and *Poly-Bio* (Fig. 1.D_1) are the main arrangements for this type of polytropic configuration; whereas *Poly-MDMD* and *Poly-DMDM* correspond to two specific arrangements in which the biogas components, CH_4 (M) and CO_2, (D) were separately fed through (h_{12}, h_6) and (h_9, h_3) respectively (Fig. 1.D_2), and vice versa (Fig. 1.D_3).

Three different types of experiments were carried out for every set of experimental conditions:

(i) long-lasting isothermal experiments for a total time-on-stream (TOS) of about 300 min at 400 ºC, maintaining the feeding configuration (i.e., working with one of the aforementioned reactor schemes – Fig. 1-). The highest temperature, 400 ºC, was selected since it is at which the reaction system is most susceptible to catalyst deactivation. This last might be due to both degradation of the catalyst structure from thermal stress

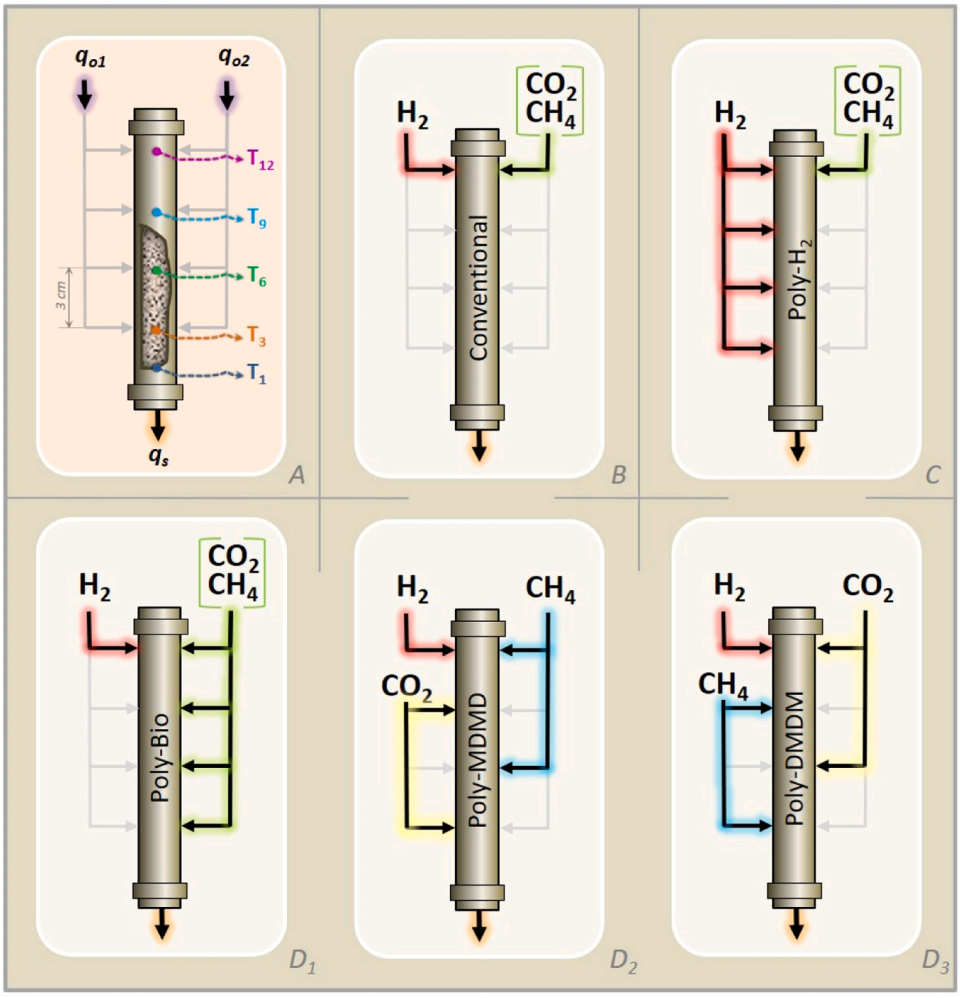

Fig. 1. Reactor sketches showing the position of thermocouples and the distribution of feed stream inlets (A). Feeding configurations: Conventional (B), Poly-H_2 (C), and Poly-Biogas (D) [including Poly-Bio (D_1), Poly-MDMD (D_2), and Poly-DMDM (D_3)].

(sintering of the active phase) and coke production (fouling of the active phase) according with the thermodynamic equilibrium.

(ii) dynamic experiments using a specific feeding configurations and varying temperatures along the time-on-stream (TOS). Temperature was set from 400 to 250 ºC (down step), in intervals of -25 °C (45 min TOS at each temperature),

(iii) finally, other isothermal dynamic experiments analogous to (*ii*) but working at constant temperature and varying the total flow rate q_0. They were carried out for each feeding configuration to determine the effect of the space velocity, *WHSV*.

The CO_2 conversion (Eq. 1), H_2 conversion (Eq. 2), and CO selectivity (Eq. 3 or Eq. 4) were evaluated to measure the configuration performances. In general, unless otherwise stated, CO selectivity will be calculated by Eq. 3 based on the total quantified amount of products (CH_4 and CO). However, in some cases an equivalent calculation (Eq. 4) based on the amount of reactive CO_2 converted will be used.

$$CO_2 conversion(\%) = \left[\frac{f_{CO_2}|_{in} - f_{CO_2}|_{out}}{f_{CO_2}|_{in}}\right] \cdot 100 \quad (1)$$

$$H_2 conversion(\%) = \left[\frac{f_{H_2}|_{in} - f_{H_2}|_{out}}{f_{H_2}|_{in}}\right] \cdot 100 \quad (2)$$

$$CO\ selectivity(\%) = \left[\frac{f_{CO}|_{out}}{f_{CH_4}|_{out} - f_{CH_4}|_{in} + f_{CO}|_{out}}\right] \cdot 100 \quad (3)$$

$$CO\ selectivity(\%) = \left[\frac{f_{CO}|_{out}}{f_{CO_2}|_{in} - f_{CO_2}|_{out}}\right] \cdot 100 \quad (4)$$

where $f_k|_{in}$ and $f_k|_{out}$ are total molar flows (mmol·min^{-1}) of compound *k* entering or leaving the reactor, respectively. On that way, molar flows of the different substances (*k*), with $f_k|_{out}$ measured by chromatographic analysis, allow to verify the balance closure for each element in reaction (i.e., C, H, and O). Thus, for example, the carbon balance closures were obtained with errors always lower than 2 % throughout the entire TOS.

3. Results and discussion

3.1. Catalyst characterization

The fresh catalyst presented a surface area of 21.1±0.1 m^2·g^{-1} (BET), an average grain size of around 1 μm (estimated from SEM observations), and Ni and Mn atomic contents of 4.6 %^{wt} and 70.1 %^{wt}, respectively (XRF). Surface Ni/(Ni+Mn) mass ratios showed an average value of 5.7 %^{wt}, obtained from EDX mapping, what revealed also a dispersed and homogeneous distribution of both Ni and Mn on the catalyst surface. Fig. 2 shows its XRD diffractograms for three stages: fresh, activated (i.e., after being reduced with H_2), and after reaction. This last pattern was obtained for a sample extracted from the bed after the experimental run, and consequently containing alumina from the packed bed. The oxides of Mn^{3+} and Mn^{2+} were the only phases observed for the fresh and the reduced catalyst, respectively. After reaction, manganese kept its reduced state (MnO) and no Mn_2O_3 peaks were observed. Moreover, peaks corresponding to nickel were not observed in any sample, which is attributed to its scarce content and/or a low crystallinity on the solid surface.

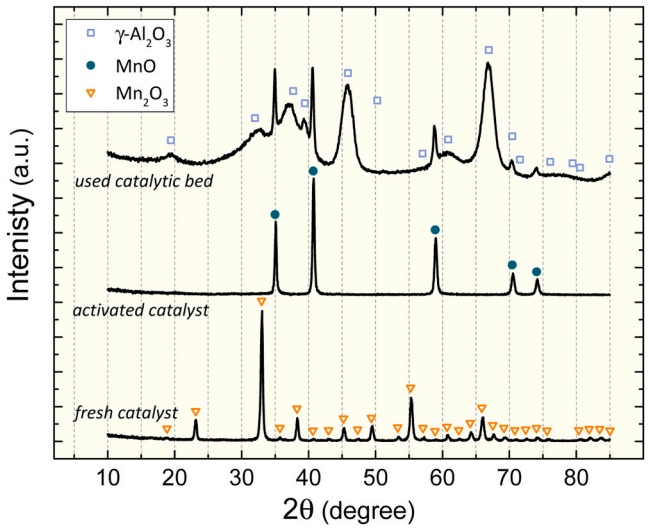

Fig. 2. XRD diffractograms for fresh, reduced (activated) catalyst, and bed's solid material (mixture of catalyst and inert particles) after reaction. Symbols for identification of crystalline phases (Mn_2O_3, MnO, and γ-Al_2O_3).

3.2. Long-lasting isothermal experiments. Stability

Although in literature it has already been reported [18] about the feasibility of carrying out the biogas upgrading through its thermocatalytic methanation in this same type of reactor, to the authors knowledge it is the first time that upgrading has been carried out in a distributed feeding mode.

This first type of experiments was carried out under reference conditions (Table 1). The aim of these isothermal five-hour lasting experiments at the highest temperature (400 ºC) was to verify the feasibility of the different proposed configurations (Fig. 1) as well as the stability of the process.

Fig. 3 presents the time evolution of CO_2 and H_2 conversions along time for the main configurations (*Conventional*, *Poly-H2*, and *Poly-Bio*). The stability of the results can be clearly appreciated. In fact, from the first 15 minutes on, no significant variation in catalytic activity can be observed.

Since the stoichiometry employed in these experiments is 4:1 for the H_2:CO_2 molar ratio, both conversion of CO_2 and of H_2 should be equal

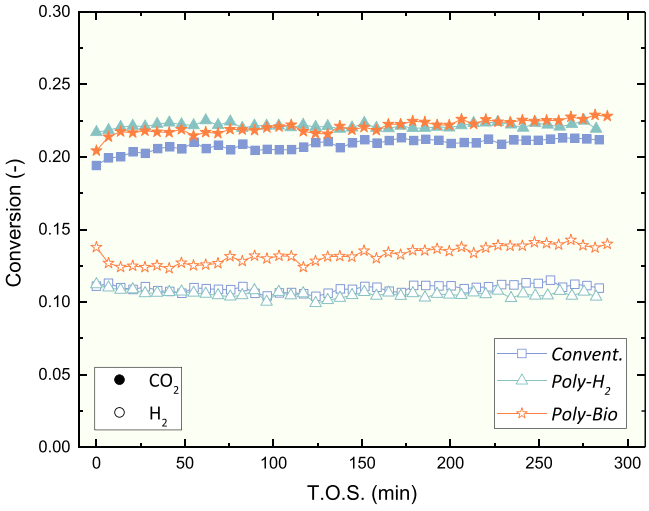

Fig. 3. Time evolution of CO_2 conversion (solid symbols) and H_2 conversion (hollow symbols) in long-lasting experiments as a function of the feeding configuration. Operating conditions: standard values (Table 1).

resembling *Sabatier* reaction (r.1). However, in view of the results, which show a greater conversion of CO_2 compared to that of H_2, it was expected the existence of relatively high selectivities towards CO for all configurations. The lower conversion of hydrogen than of carbon dioxide reveals the formation of carbon monoxide through the reverse *Water Gas Shift* reaction (r.2) without its subsequent transformation to methane through the reverse *Methane Steam Reforming* (r.3).

Poly-Bio configuration shows a noticeably higher H_2 conversion than in the other cases, while maintaining a similar carbon dioxide conversion. This result anticipates a lower selectivity to CO with the same carbon dioxide conversion for this configuration, which would coincide with the previously mentioned assumed hypothesis.

A post-mortem catalyst sample, from two sets of consecutive experiments (a seven-temperature dynamic experiment followed by a long-term isothermal experiment for 6 h at 400 ºC), both with *Poly-Bio* feeding configuration, $W_{cat,0} = 0.125$ g and the rest of the conditions at their standard values (Table 1), were separated and taken for characterization. Raman spectroscopy was performed on a *WiTecAlpha300 confocal Raman microscope* and TPO analysis was performed on a *Netzsch® STA 449 F3 Jupiter* thermogravimetric analyzer connected to an *Omnistar GSD301 01 Pfeiffer* vacuum mass spectrometer. The results did not reveal any significant presence of carbonaceous residues on the catalyst surface, which corroborates the good C-balance closures and the stability of the reaction experiments.

3.3. T-dynamic experiments

3.3.1. Methanation at different temperatures

This type of dynamic experiments in which temperature is varied every time lapse of ca. 45 min, let know the performance and stability of the process (through H_2 and CO_2 conversions), as well as verifies that it is working with weight-related space velocities (*WHSV*) high enough to keep distant from thermodynamic equilibrium at any of the temperatures in the chosen range (250–400 ºC).

Fig. 4 shows the results for a T-dynamic experiment that could be considered an example of performance. For a given reactor feeding configuration (in this case, *Poly-Bio*), all operating conditions were fixed including the WHSV and a preprogrammed dynamic temperature variation with time-on-stream: T_6 (controlling thermocouple 6 cm above the distribution plate) was varied from 400 to 250 ºC decreasing 25 ºC every 45 min. Stable temperature values were quickly reached at each step, exception made of the segment at the beginning of the experiment, when working at 400 ºC. In this case, a slightly different behavior is appreciated characterized by an initial large rise in temperature due to the exothermicity of the process, producing a peak (marked as ΔT_{max}). This leads the system to a later stabilization than in subsequent stages.

Likewise, regarding the evolution of CO_2 and H_2 conversions, they also stabilize at each stage as soon as the temperature does. Achieved conversion values in each segment (i.e., temperature) were always far from those corresponding to the thermodynamic equilibrium (represented in Fig. 4 with horizontal red lines). Moreover, mass balance closures were always close to 100 %. So, these data can be appropriately used in the analysis of results.

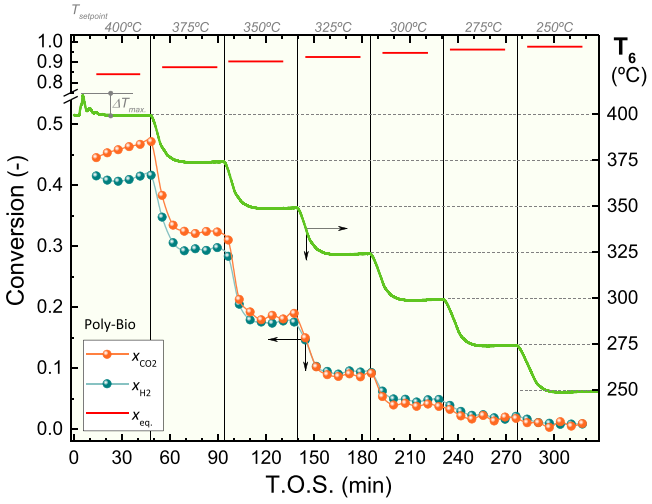

Fig. 4. CO_2 and H_2 conversions and temperature T_6 as a function of time-on-stream (TOS) for a standard run working with *Poly-Bio* configuration. Operating conditions: standard values (Table 1) and $W_{cat,0} = 0.50$ g, $W_{inert,0} = 10.0$ g, *WHSV* = 6.63 $g_{CO2} \cdot g_{cat}^{-1} \cdot h^{-1}$. T = 400 – 250 ºC. Horizontal red lines represent thermodynamic equilibrium conversions at each set-point temperature.

3.3.2. Selectivity vs. conversion: effect of the feeding configuration

Fig. 5 shows the comparison of selectivity to CO *vs.* CO_2 conversion curves for the five feeding configurations tested in the *T*-dynamic runs operating at the reference conditions (Table 1).

Similar trends have been found for all feeding configurations at temperatures of 300 ºC and above. As expected, when considering the selectivity towards an intermediate product, in this case CO, in a process constituted by reactions in series (i.e., (r.2) and (r.3)), selectivity towards CO decreases when CO_2 conversion increases. However, despite the qualitative similitudes, the current values of pairs CO selectivity – CO_2 conversion are quite different depending on the configuration. Thus, as shown in Fig. 5, for any conversion using *Poly-Biogas* configuration (i.e., *Poly-Bio*, *Poly-DMDM*, and *Poly-MDMD*), results are always less selective to CO than those obtained for *Conventional* or *Poly-H_2* ones. For example, when x_{CO2} = 19 %, selectivities to CO decrease in the sequence: *Conventional*> *Poly-H_2* > *Poly-DMDM*> *Poly-Bio*> *Poly-MDMD* (selectivity values of 64.0 %, 60.2 %, 48.8 %, 40.9 %, and 21.9 %, respectively). Therefore, by separately distributing the CO_2 and CH_4 feeds (*DMDM* or *MDMD*) between the various inlets of the reactor (see Fig. 1.D_2 and 1.D_3), CO selectivities are obtained with different values but around those of the *Poly-Bio* configuration. All these effects on selectivity are consistent with a series-parallel reaction scheme in which H_2 acts as an attacking reagent on CO_2. Consequently, the route consisting of rWGS (r.2) and subsequent rMSR (r.3) hydrogenation reactions in series, apparently dominates this specific Ni-Mn catalytic process.

Additionally to being more selective to the valued product (CH_4), at any working temperature *Poly-Bio* arrangement is always more active than the *Conventional* or the *Poly-H_2* ones. For example, at 375ºC the

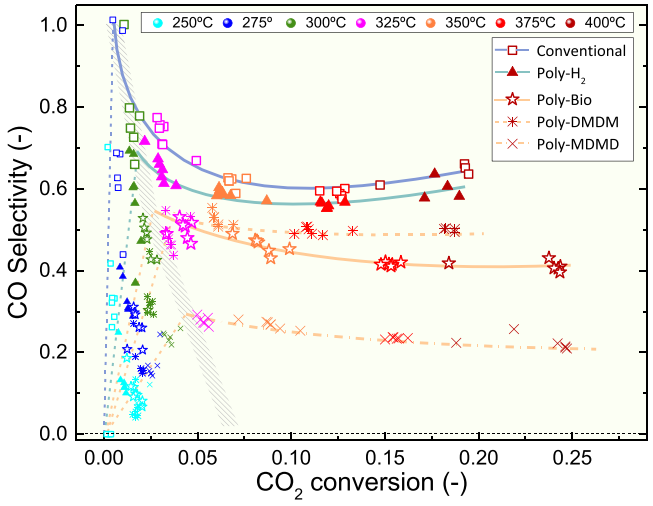

Fig. 5. Selectivity to CO vs. CO_2 conversion as a function of the temperature set-point (represented with different colors) and the feeding configuration (represented with different symbols). Operating conditions: standard values (Table 1). T = 400 – 250 ºC. Curves only for visual guidance.

average values of conversion are $\bar{x}_{CO2}$ = 12.5 % for *Conventional* and $\bar{x}_{CO2}$ =15.3 % for *Poly-Bio*. The same trend is seen for the rest of temperatures in the analyzed range (300–400 ºC). The hypothesis is that the higher conversions obtained with *Poly-Bio* configuration, compared to *Conventional* or *Poly-H*$_2$, can be attributed to a spreading of the reaction zone by distributing the CO_2 (in series - reagent in (r.2) and (r.3)) along the axial dimension of the bed. In such way, the active part of the catalytic bed covers a greater fraction of its height.

Summing up, in the range from 300 ºC to 400ºC the best results in activity (higher conversion at the same temperature) and selectivity (lower selectivity to CO at iso-conversion) are always clearly found for distributed biogas feeds (*Poly-Biogas*). In this sense, the working hypothesis for biogas methanation is confirmed and coincides with what was obtained for CO_2 methanation [4].

Considering now the results of selectivity versus conversion for the low temperatures range (250–300 ºC) in Fig. 5, a clear decreasing trend in CO selectivity is observed when CO_2 conversion drops. In the limit, selectivity tends to null values. This trend would be favorable for the biogas upgrading in terms of selectivity, since it leans towards a totally selective process with CH_4 as single product, but not in terms of activity given the very low CO_2 conversions attained in this range. Moreover, it was actually unexpected and differs from what was found for the methanation of CO_2 [10]. In fact, when comparing the current results with the previous ones corresponding to the methanation of CO_2 (i.e., without CH_4 in the fed stream), the difference is clear. It can be seen, in Fig. 6, for the specific case of the *Poly-Bio* configuration versus its equivalent *Poly-CO*$_2$ obtained when there was not CH_4 in the inlet.

In Fig. 6 for CO_2 conversions greater than approximately 5 %, biogas processing by feeding in a distributed manner (*Poly-Bio*) leads to a selectivity vs. conversion curve like that obtained with the distribution of CO_2 (*Poly-CO*$_2$). Thus, the presence of CH_4 in the feed apparently does not represent a penalty in terms of selectivity or activity. In fact, even slightly higher conversions are obtained at different temperatures with the *Poly-Bio* configuration. In the zone of very low conversions (x_{CO2} < 5 %), which would not be very viable from a practical point of view, on the one hand processing biogas would lead to the complete methanation of that paltry amount of reacted CO_2; on the other, processing only CO_2 would result in the intermediate product CO as the single final one. The calculation of selectivity to CO, carried out with Eq. (3), is susceptible to producing a significant error since its denominator involves the subtraction of two high values corresponding to $f_{CH_4}|_{in}$ and $f_{CH_4}|_{out}$. Therefore, selectivity was also calculated with the equivalent Eq. (4), which does not use such magnitudes. Nevertheless, the resulting selectivity values and shape of the curve were analogous to those obtained with Eq. (3), and already shown in Fig. 6, which allowed this problem to be ruled out.

3.3.3. Selectivity vs. conversion: effect of space velocity

Up to this point the changes in conversion were achieved by modifying the temperature through T-dynamic experiments, keeping the rest of the conditions constant at their standard values (Table 1), and therefore at a constant *WHSV* value of 13.25 $g_{CO2}{\cdot}g_{cat}^{-1}{\cdot}h^{-1}$). The T-dynamic experiments were repeated for all feeding configurations doubling the amount of catalyst in the bed ($W_{cat,0}$ = 0.50 g) and therefore with a space velocity half of the previous one. Fig. 7 shows the compared results of both series for the *Conventional* and *Poly-Bio* configurations. As expected, for a specific feeding configuration, decreasing space velocity (i.e. going from hollow symbols to solid ones) leads to increased conversion at all temperatures. Additionally, regardless of the space velocity selected, the *Poly-Bio* configuration (star symbols) leads to higher CO_2 conversion and lower CO selectivity than the conventional configuration (square symbols). This is true not only for the zone of high temperatures and conversions, but over the entire range, even with x_{CO2} < 5 % and temperatures of 250 ºC or 275 ºC.

3.4. WHSV-dynamic experiments

Temperature (*T*) may produce a great influence on the selectivity toward the intermediate product CO. The reason can be found in that large differences between activation energies of the methanation reactions ((r.2) and (r.3)) may lead to a different evolution of its kinetics, and therefore, of selectivity.

To decouple the effect of *T* on the selectivity vs. conversion curves, a new series of experiments was carried out. This series used standard values (Table 1) and a different catalyst loading ($W_{cat,0}$ = 0.125 g). For checking purposes, the total gas flow rate was decreased in steps, starting from an initial value of q_0 = 450 STP mL/min until q_0 = 62.5 STP mL/min, every 60 min TOS duration. That represents a reduction in *WHSV* from 47.71 $g_{CO2}{\cdot}g_{cat}^{-1}{\cdot}h^{-1}$ to 6.63 $g_{CO2}{\cdot}g_{cat}^{-1}{\cdot}h^{-1}$.

Fig. 8 shows the isothermal (400 ºC) variation of the selectivity to CO vs. CO_2 conversion curves for *Conventional*, *Poly-Bio*, and *Poly-H*$_2$ feeding configurations. In this case, the CO selectivity values have been

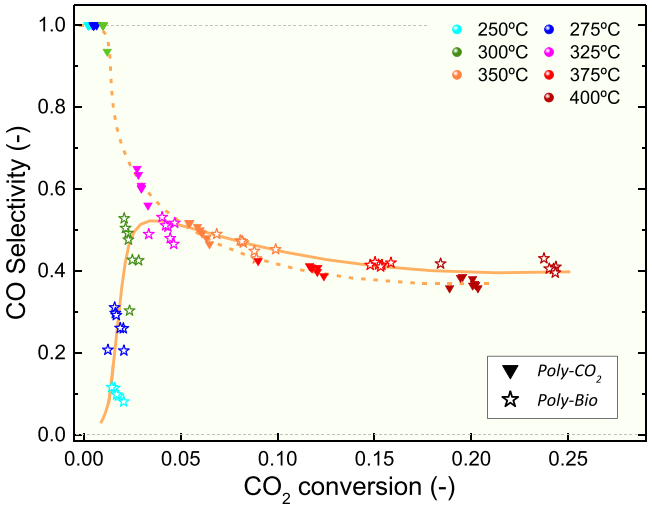

Fig. 6. Selectivity to CO vs. CO_2 conversion for the polytropic feeding configuration as a function of the temperature set-point, for both CO_2 [10] or biogas methanation experiments. Operating conditions: standard values (Table 1). *T* = 400 – 250 ºC represented with different colors. Lines only for visual guidance. Solid symbols: *Poly-CO*$_2$; Hollow symbols: *Poly-Bio*.

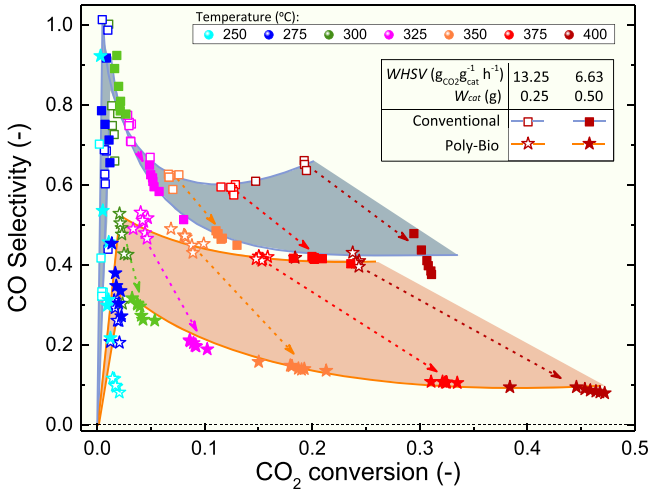

Fig. 7. Selectivity to CO vs. CO_2 conversion as a function of the temperature set-point and the feeding configuration (*Conventional* and *Poly-Bio*), for two different *WHSV* values. Operating conditions: standard values (Table 1). *WHSV*: 13.25 or 6.63 $g_{CO2}{\cdot}g_{cat}^{-1}{\cdot}h^{-1}$. Colored areas and lines only for visual guidance (slashed arrows ticking the effect of decreasing *WHSV*).

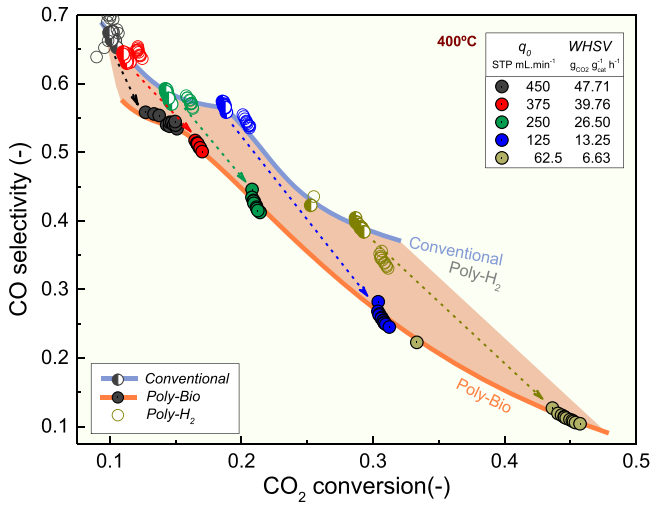

Fig. 8. Selectivity to CO vs. CO_2 conversion as a function of the *WHSV* and the feeding configuration (*Conventional*, *Poly-Bio*, and *Poly-H$_2$*). Operating conditions: standard values (Table 1), but $W_{cat,0}$= 0.125 g. *WHSV*: 47.71 – 6.63 $g_{CO2}·g_{cat}^{-1}·h^{-1}$ (q_0= 450 – 62.5 (STP)mL·min^{-1}). Colored area and curves only for visual guidance (slashed arrows ticking the effect of changing feeding configuration at same *WHSV*).

calculated using Eq. (4). Logically, decreasing *WHSV* results in an increase in conversion, regardless of the feeding configuration used. For identical operating conditions but, unlike in the previous sections, now including also the same temperature (same color symbols), the *Poly-Bio* configuration (solid symbols) leads to higher activity (i.e., greater CO_2 conversion) and lower selectivity towards CO than both the *Poly-H$_2$* and *Conventional* configurations (hollow and semi-hollow symbols respectively), these last two configurations offering similar results each other.

Summing up, the reactor with distributed biogas feeding (*Poly-Bio*) confirms its greater efficiency and better selectivity for biogas upgrading also when working in isothermal conditions. For example, by setting a conversion x_{CO2} = 30 % the *Poly-Bio* reactor allows more than double the processing capacity of the *Conventional* reactor (a *WHSV* ≥ 13.25 $g_{CO2}·g_{cat}^{-1}·h^{-1}$ is required for *Poly-Bio* configuration versus a *WHSV*< 6.63 $g_{CO2}·g_{cat}^{-1}·h^{-1}$ for the *Conventional* one, Fig. 8). Furthermore, under these conditions (CO selectivity values of 27.2 % and 38.5 %, respectively), the methane production ($g_{CH4}·min^{-1}$) from the *Poly-Bio* configuration will be 2.37 times that obtained from the *Conventional* configuration.

3.5. Temperature profiles

In addition to improving activity and selectivity, a thermal effect was also sought when the side distribution of the feed stream was carried out. In fact, it was sought to mitigate the negative effects of such a strongly exothermic reaction (*Sabatier*'s (r.1)), both in terms of avoiding generation of hot spots and in softening of the axial temperature profiles along the bed.

The parameter ΔT_{max} has been defined as the maximum difference between the temperature measured along the axial dimension of the bed in the five axial positions (T_1, T_3, T_6, T_9 and T_{12}) and the temperature set-point (T_6). Fig. 9A shows the specific temperature increases ΔT_{max} occurring at the beginning of the reaction under standard conditions (see first minutes of Fig. 4). It shows values for different bed heights, and for the three feeding configurations. They are also compared with those formerly obtained for CO_2 methanation [10]. Unlike what happened with CO_2 methanation (symbols), the ΔT_{max} profiles in biogas methanation (bars) do not present a clear trend regardless of the feeding configuration, being always much lower than those for CO_2

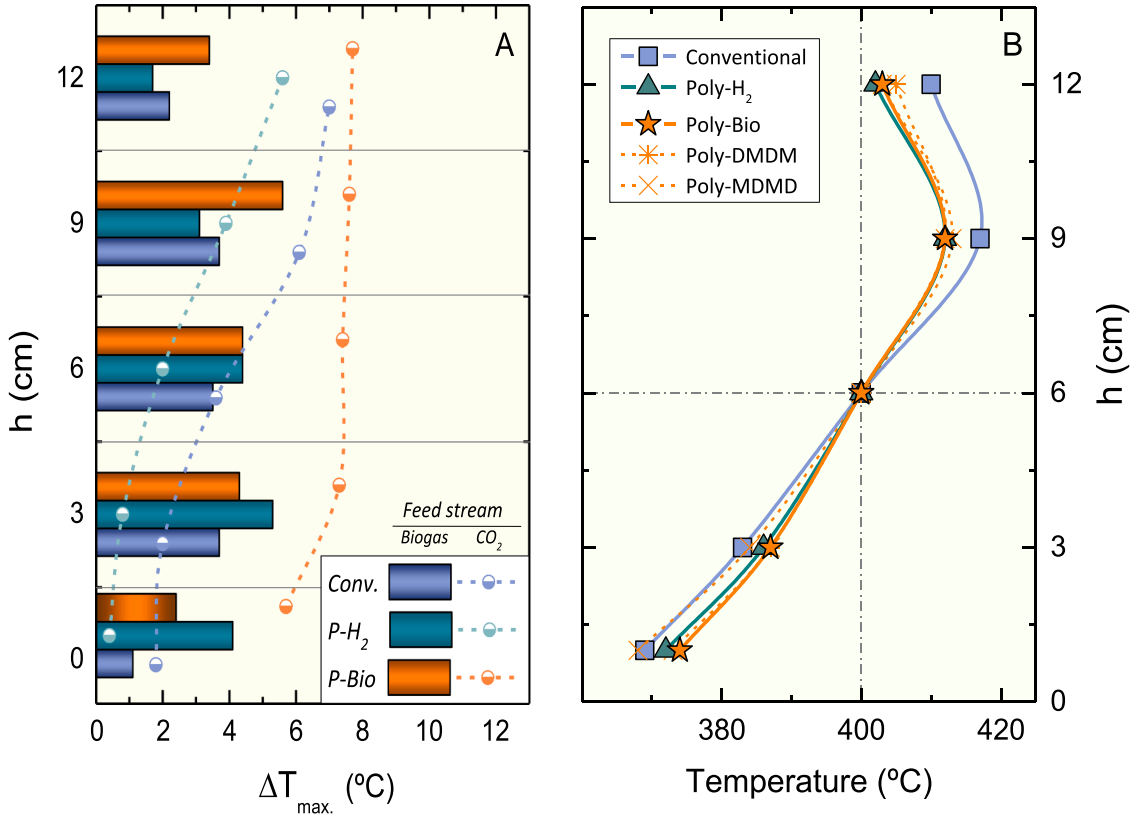

Fig. 9. Thermal effect profiles in the packed bed for the different feeding configurations: A) maximum temperature increase (ΔT_{max}) profiles (bars represent runs feeding biogas and symbols feeding only CO_2), and B) stable temperature profiles. Standard operating conditions (Table 1). Curves only for visual help.

hydrogenation. *Poly-Bio* configuration does not exhibit a more homogeneous ΔT_{max} profile than that for *Poly-CO_2*. Furthermore, in general terms the ΔT_{max} values are lower for biogas methanation (around +4ºC) than that there were for CO_2. This behavior can be attributed to the dilution of the CO_2 reagent in biogas due to its methane content (current molar fraction $|y_{CO_2}|_{biogas} = 0.12$ instead of $|y_{CO_2}|_{CO_2} = 0.18$), so that the heat generation per volume unit in the bed is roughly 33 % lower with the same conversion.

On the other hand, Fig. 9B shows the steady state temperature profiles obtained for the standard experiments with all the feeding configurations tested in this work for biogas methanation. Although the effect is not as great as it could be, due to the already mentioned implicit dilution of CO_2 in the biogas, a clear softening effect can be seen in the temperature profiles when there is a side distribution of the feed. Thus, the profile furthest from isothermicity is presented by the *Conventional* configuration, while for the others, especially for the *Poly-Bio*, there is a less pronounced temperature profile that tends to isothermicity along the catalytic bed. In short, as also discussed elsewhere [19], a more homogeneous temperature profile could be achieved in the bed without increasing the severity of hot-spots, by adopting a *Poly-Bio* (or *Poly-CO_2*) feeding configuration.

4. Conclusions

A feasible and stable (up to at least a TOS = 300 min) biogas upgrading has been observed by its methanation in the Ni-Mn catalytic fixed bed, regardless of the feeding configuration and working temperature adopted.

There are large differences between the 'CO selectivity versus CO_2 conversion' curves obtained for different reactor feeding configurations at constant weight hourly space velocity *WHSV* and variable temperatures (*T*-dynamic experiments). For any CO_2 conversion, *Poly-biogas* feeding configurations leads always to a better performance (i.e., lower CO selectivities at a given CO_2 conversion) than either *Conventional* or *Poly-H_2*. Comparing these results with their equivalents previously obtained for CO_2 methanation [10], the curves are similar. Thus, for example, the *Poly-Bio* curves are similar to those obtained with the distribution of CO_2 (*Poly-CO_2*). A different behavior is only obtained in the range of very low CO_2 conversions, below x_{CO2}=5 %. Furthermore, for different feeding configurations there is a similar relative order between them, in terms of CO selectivity at iso-CO_2 conversion (i.e., *Poly-CO_2* is the least CO selective feeding configuration).

Working at constant temperature (*WHSV*-dynamic experiments), distributed biogas feeding (*Poly-Bio*) confirms its greater efficiency and better selectivity for biogas upgrading. Thus, operating the fixed bed reactor in *Poly-Bio* feeding mode can give a methane production rate ($g_{CH4}{\cdot}min^{-1}$) more than twice that obtained in a *Conventional* configuration working with the same operating conditions (*T*, *WHSV*, $H_2 : CO_2|_{in}$ ratio, $CH_4 : CO_2|_{in}$, pressure, etc …)

Finally, early temperature hot spots appearance coming from intense reaction in zones close to the entrance of reactants are significatively lower for biogas methanation than for CO_2 methanation. Furthermore, by adopting a *Poly-Bio* feeding configuration a more homogeneous temperature profile is obtained in the bed.

Consequently, acting on the feed configuration in the fixed-bed catalytic reactor could be an interesting way to improve its performance for the Power to Gas (PtG) strategy, and specifically for the biogas upgrading.

CRediT authorship contribution statement

José Ángel Peña:Writing – review & editing, Validation, Supervision, Resources, Methodology, Funding acquisition, Conceptualization. **Eva Francés**:Writing – review & editing, Supervision, Data curation. **Fernando Cazaña**:Resources. **Víctor Daniel Mercader**:Writing – review & editing, Data curation. **Javier Herguido**:Writing – review & editing, Writing – original draft, Visualization, Validation, Supervision, Methodology, Investigation, Conceptualization. **Rodrigo González-Pizarro**:Investigation, Data curation. **Pablo Aragüés-Aldea**:Investigation, Data curation. **Paul Durán**:Methodology, Investigation, Data curation

Declaration of Competing Interest

The authors declare that they have no known competing financial interests or personal relationships that could have appeared to influence the work reported in this paper.

Data Availability

Data will be made available on request.

Acknowledgements

This research was funded by MICINN (*Spanish Ministerio de Ciencia e Innovación*) projects number PID2019–104866RB-I00, PID2020–113809RB-C31, and PID2022–136947OB-I00. In addition, the consolidated research group Catalysis and Reactor Engineering Group (CREG) (T43–23R) has the financial support of *Gobierno de Aragón* (Aragón, Spain) through the European Social Fund – FEDER. Also V.D. Mercader and P. Aragüés-Aldea want to express their gratitude for the research grants of *Ministerio de Ciencia e Innovación* (VDM) (grant no. PRE2020–095679) and *Gobierno de Aragón* (PAA) respectively. Finally, authors would also like to acknowledge the use of *Servicio General de Apoyo a la Investigación-SAI* (Universidad de Zaragoza).

References

[1] D. Rusmanis, Y. Yang, R. Lin, D.M. Wall, J.D. Murphy, Operation of a circular economy, energy, environmental system at a wastewater treatment plant, Adv. Appl. Energy 8 (2022) 100109, https://doi.org/10.1016/j.adapen.2022.100109.

[2] M. Bailera, P. Lisbona, L.M. Romeo, S. Espatolero, Power to gas projects review: lab, pilot and demo plants for storing renewable energy and CO_2, Renew. Sustain. Energy Rev. 69 (2017) 292–312, https://doi.org/10.1016/j.rser.2016.11.130.

[3] M. Götz, J. Lefebvre, F. Mörs, A.M. Koch, F. Graf, S. Bajohr, R. Reimert, T. Kolb, Renewable power-to-gas: a technological and economic review, Renew. Energy 85 (2016) 1371–1390, https://doi.org/10.1016/j.renene.2015.07.066.

[4] Z. Liu, X. Gao, K. Wang, J. Liang, Y. Jiang, Q. Ma, T.-S. Zhao, J. Zhang, A short overview of power-to-methane: coupling preparation of feed gas with CO_2 methanation, Chem. Eng. Sci. 274 (2023) 118692, https://doi.org/10.1016/j.ces.2023.118692.

[5] G. Varvoutis, M. Lykaki, S. Stefa, V. Binas, G.E. Marnellos, M. Konsolakis, Deciphering the role of Ni particle size and nickel-ceria interfacial perimeter in the low-temperature CO_2 methanation reaction over remarkably active Ni/CeO_2 nanorods, Appl. Catal. B Environ. 297 (2021) 120401, https://doi.org/10.1016/j.apcatb.2021.120401.

[6] A.I. Tsiotsias, N.D. Charisiou, E. Harkou, S. Hafeez, G. Manos, A. Constantinou, A. G.S. Hussien, A.A. Dabbawala, V. Sebastian, S.J. Hinder, M.A. Baker, K. Polychronopoulou, M.A. Goula, Enhancing CO_2 methanation over Ni catalysts supported on sol-gel derived Pr_2O_3-CeO_2: an experimental and theoretical investigation, Appl. Catal. B Environ. 318 (2022) 121836, https://doi.org/10.1016/j.apcatb.2022.121836.

[7] Z. Boukha, A. Bermejo-López, U. De-La-Torre, J.R. González-Velasco, Behavior of nickel supported on calcium-enriched hydroxyapatite samples for CCU-methanation and ICCU-methanation processes, Appl. Catal. B Environ. 338 (2023) 122989, https://doi.org/10.1016/j.apcatb.2023.122989.

[8] C. Larghi, A. Porta, C.G. Visconti, L. Lietti, Intensification of Ru/Al_2O_3 Catalysts for CO_2 Methanation" in *28th North American Catalysis Society Meeting (NAM28)*, Providence R.I. – USA- June 2023. ⟨https://nam.confex.com/nam/2023/meetingapp.cgi/Paper/32235⟩.

[9] C. Larghi, A. Porta, R. Matarrese, C.G. Visconti, L. Lietti, CO_2 Methanation Over Ru and Ni Based Catalysts: Towards a Comprehensive Kinetic Model through a Multi-Technique Study" in *15th European Congress on Catalysis (Europacat 2023)*, Prague - Czech Repuclic. August-September 2023. Book of abstracts. ⟨https://www.europacat2023.cz/Amca-Europacat2021/media/content/Docs/Book_of_abstracts-EuropaCat2023.pdf⟩.

[10] P. Aragüés-Aldea, A. Sanz-Martínez, P. Durán, E. Francés, J.A. Peña, J. Herguido, Improving CO_2 methanation performance by distributed feeding in a Ni-Mn catalyst fixed bed reactor, Fuel 321 (2022) 124075, https://doi.org/10.1016/j.fuel.2022.124075.

[11] J. Santamaría, M. Menéndez, J.A. Peña, J.I. Barahona, Methane oxidative coupling in fixed bed catalytic reactors with a distributed oxygen feed. A simulation study, Catal. Today 13 (1992) 353–360, https://doi.org/10.1016/0920-5861(92)80160-O.

[12] N.D. Charisiou, G. Siakavelas, L. Tzounis, V. Sebastian, A. Monzon, M.A. Baker, S. J. Hinder, K. Polychronopoulou, I.V. Yentekakis, M.A. Goula, An in-depth investigation of deactivation through carbon formation during the biogas dry reforming reaction for Ni supported on modified with CeO_2 and La_2O_3 zirconia catalysts, Int. J. Hydrog. Energy 43 (2018) 18955–18976, https://doi.org/10.1016/j.ijhydene.2018.08.074.

[13] Y. Gao, A. Aihemaiti, J. Jiang, Y. Meng, T. Ju, S. Han, X. Chen, J. Liu, Inspection over carbon deposition features of various nickel catalysts during simulated biogas dry reforming, J. Clean. Prod. 260 (2020) 120944, https://doi.org/10.1016/j.jclepro.2020.120944.

[14] A.C. Faria, C.V. Miguel, L.M. Madeira, Thermodynamic analysis of the CO_2 methanation reaction with in situ water removal for biogas upgrading, J. CO2 Util. 26 (2018) 271–280, https://doi.org/10.1016/j.jcou.2018.05.005.

[15] X.J. Merchán. Development of CO_2 Methanation Catalysts from Lignocellulosic Residues, Universidad de Zaragoza, Zaragoza (Spain), 2019.

[16] P. Tarifa, C. Megías-Sayago, F. Cazaña, M. González-Martín, N. Latorre, E. Romeo, J.J. Delgado, A. Monzón, Highly active Ce- and Mg-promoted Ni catalysts supported on cellulose-derived carbon for low-temperature CO_2 methanation, Energy Fuels 35 (2021) 17212–17224, https://doi.org/10.1021/acs.energyfuels.1c01682.

[17] Y. Wei, S. Li, J. Jing, M. Yang, C. Jiang, W. Chu, Synthesis of Cu–Co catalysts for methanol decomposition to hydrogen production via deposition–precipitation with urea method, Catal. Lett. 149 (2019) 2671–2682, https://doi.org/10.1007/s10562-019-02731-9.

[18] A. Sanz-Martínez, P. Durán, V.D. Mercader, E. Francés, J.Á. Peña, J. Herguido, Biogas Upgrading by CO_2 methanation with Ni-, Ni–Fe-, and Ru-Based Catalysts, Catalysts 12 (12) (2022) 1609, https://doi.org/10.3390/catal12121609.

[19] P. Durán, I. Esteban, E. Francés, J.A. Peña, J. Herguido, Use of A Fixed Bed Reactor with Distributed Feed to Minimize Thermal Gradients for Synthetic Natural Gas Production, First Int. Conf. Unconv. Catal. React. Appl., Zaragoza (Spain), 2019.